Generating n-Scroll Chaotic Attractors From A Memristor-based Magnetized Hopfield Neural Network

Hairong Lin, *Member, IEEE*, Chunhua Wang, Yichuang Sun, *Senior Member, IEEE*, and Ting Wang

***Abstract*—This brief presents a novel method to generate n-scroll chaotic attractors. First, a magnetized Hopfield neural network (HNN) with three neurons is modeled by introducing an improved multi-piecewise memristor to describe the effect of electromagnetic induction. Theoretical analysis and numerical simulation show that the memristor-based magnetized HNN can generate multi-scroll chaotic attractors with arbitrary number of scrolls. The number of scrolls can be easily changed by adjusting the memristor control parameters. Besides, complex initial offset boosting behavior is revealed from the magnetized HNN. Finally, a magnetized HNN circuit is designed and various typical attractors are verified.**

***Index Terms*—Memristor, Hopfield neural network, multi-scroll attractor, initial offset boosting, circuit implementation.**

I. Introduction

SINCE Lorenz found the first chaotic attractor in 1963 [1], scientists have done extensive investigations in the chaotic attractors [2, 3]. Among them, the most important research is to generate chaotic attractors. Due to their adjustability and high complexity, the multi-scroll chaotic attractors can be widely applied in chaos control [4] and image encryption [5]. Consequently, the research on the construction of chaotic systems with multi-scroll attractors has attracted much attention from many scholars internationally.

Over the past few decades, there have been many work devoted to constructing multi-scroll chaotic systems. From a survey of the literature, there are three major methods: 1) Constructing multi-scroll chaotic systems based on Chua's circuit [6]. Especially, in 2018, Hong *et al*. presented a multi-direction multi-double-scroll chaotic system based on Chua's circuit adopting a pulse control method [7]. Based on an improved Chua's circuit with a piecewise-linear diode, Wang *et al*. constructed a multi-scroll chaotic system in 2019 [8]. In 2021, Zhang *et al*. designed a chaotic system with multi-double-scroll attractors by introducing a piecewise-nonlinear memristor into a Chua's circuit [9]. 2) Constructing multi-scroll chaotic systems based on Jerk-like systems [10]. For instance, in 2019, by using a nonlinear function shift method, Hong *et al*. proposed a multi-double-scroll chaotic system based on a modified Jerk system [11]. In 2020, Wang *et al*. designed a multi-scroll chaotic system by introducing a nested sin-PWL function into a Jerk system [12]. In 2021, Yang *et al*. constructed a sine chaotic system with multi-scroll attractors based on an improved Jerk system [13]. 3) Constructing multi-scroll chaotic systems based on other chaotic systems [14]. For example, in 2019, Wang *et al*. presented a four-dimensional multi-scroll chaotic system with four signum function series [15]. In 2021, Zhang *et al*. discovered hidden multi-scroll attractors from a modified Sprott A system with a coupling memristor [16]. In 2022, Yan *et al*. constructed a fractal multi-scroll chaotic system via fractal transformation [17].

To sum up, various multi-scroll chaotic systems have been constructed based on some special nonlinear circuits and systems. However, the generation of multi-scroll attractors based on neural networks has rarely been studied. Back in 1997, Suykens and Chua claimed that they obtained multi-double-scroll attractors from a cellular neural network [18]. Unfortunately, the trajectory and number of scrolls are neither clear nor controllable. As we all know, the HNN is a kind of nonlinear system with abundant dynamics [19]. Recently, various chaotic attractors like hyperchaotic attractors [20, 21] and coexisting attractors [22, 23] have been reported in various HNNs. Particularly, in 2020, Lin *et al*. obtained 4- and 6-scroll attractors from an HNN with three neurons [24]. Adopting a memristor synapse, Zhang *et al*. modified HNN to generate multi-scroll attractors owning even number of scrolls [25]. Furthermore, in 2022, Lai *et al*. presented the implementation of multi-double-scroll attractors from a memristive HNN with adjustable memductance [26]. Nonetheless, the multi-scroll attractors with arbitrary number of scrolls have not been found from HNNs.

In this brief, we constructed an n-scroll chaotic system based on a magnetized HNN. We first constructed a magnetized HNN model with three neurons under electromagnetic radiation. Research results show that the magnetized HNN can generate multi-scroll attractors with any number of scrolls. The number of scrolls can be easily modulated by changing control parameters. Moreover, the magnetized HNN exhibits complex initial offset boosting behavior. Finally, we designed an analog HNN circuit to demonstrate various numerical simulation results.

II. Magnetized Hopfield Neural Network

In this section, a magnetized memristive neural network is proposed based on the HNN and multi-piecewise memristor. Then its equilibrium points and corresponding stabilities are analyzed.

A. Model Description

HNN is a powerful artificial neural network, which can be described by a set of differential equations: [19]

$$C_i\dot{x}_i = -\frac{x_i}{R_i} + \sum_{j=1}^{n} w_{ij}\tanh(x_j) + I_i \quad (i, j \in N^*), \tag{1}$$

where x_i is the membrane potential of the neuron i. C_i and R_i are corresponding membrane capacitance and membrane resistance, respectively. w_{ij} stands for the coupling strength from neuron j to neuron i, namely, synaptic weight coefficients. Besides, tanh(.) and I_i represent the neuron activation function and external input current, respectively. Usually, to simplify the calculation, the values of C_i, R_i, I_i are set as 1, 1 and 0, respectively. According to model (1) and selecting suitable w_{ij}, a novel HNN with three neurons can be constructed as shown in Fig.1. Its mathematical expression is written by

$$\begin{cases} \dot{x}_1 = -x_1 + 2\tanh(x_1) - 0.8\tanh(x_2) + 0.7\tanh(x_3) \\ \dot{x}_2 = -x_2 + 3.5\tanh(x_1) + 1.6\tanh(x_2) + 1.5\tanh(x_3) \\ \dot{x}_3 = -x_3 - 2.6\tanh(x_1) + 1.2\tanh(x_2) + \tanh(x_3) \end{cases}, \tag{2}$$

Manuscript received May 9, 2022; This work is supported by the National Natural Science Foundation of China (62201204, 61971185), the China Postdoctoral Science Foundation (2022M71104), the Natural Science Foundation of Hunan Province (2020JJ4218). (*Corresponding author: Chunhua Wang.*)

Hairong Lin, Chunhua Wang are with the College of Computer Science and Electronic Engineering, Hunan University, Changsha, 410082, China. (wch1227164@hnu.edu.cn)

Yichuang Sun is with the School of Engineering and Computer Science, University of Hertfordshire, Hatfield AL10 9AB, U.K.

Ting Wang is with the School of Business Administration, Hunan University of Finance and Economics, Changsha 410205, China.

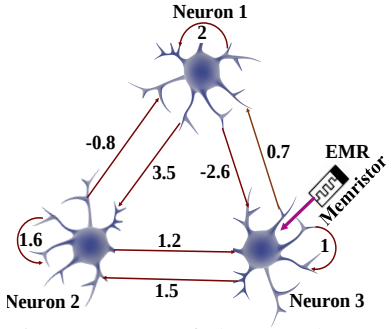

Fig. 1: Connection structure of the neural network with three neurons.

where x_i (i=1, 2, 3) is the membrane potentials of neurons i.

As shown in Fig.1, assuming neuron 3 is exposed to electromagnetic radiation (EMR). The influence of electromagnetic radiation on neurons can be described by an electromagnetic induction current generated by a flux-controlled memristor [24]. Here, an improved multi-piecewise flux-controlled memristor is introduced as follows

$$\begin{cases} i = W(\varphi)v \\ \dot{\varphi} = cv - dh(\varphi) \\ W(\varphi) = a + b|\varphi| \end{cases}, \tag{3}$$

where a, b, c and d are four parameters. $W(\varphi)$ and $h(\varphi)$ are memductance and internal state variable function of the memristor model, respectively. The $h(\varphi)$ can be written as [25]

$$h(\varphi) = \begin{cases} h_1(\varphi) = \begin{cases} \varphi, N = 0 \\ \varphi - \sum_{i=1}^{N} (\mathrm{sgn}(\varphi + (2i-1)) + \mathrm{sgn}(\varphi - (2i-1))) \\ N = 1,2,3,\ldots \end{cases} \\ h_2(\varphi) = \begin{cases} \varphi - \mathrm{sgn}(\varphi), M = 0 \\ \varphi - \mathrm{sgn}(\varphi) - \sum_{j=1}^{M} (\mathrm{sgn}(\varphi + 2j) + \mathrm{sgn}(\varphi - 2j)) \\ M = 1,2,3,\ldots \end{cases} \end{cases} \tag{4}$$

where N and M are memristor control parameters. Compared with other memristor models, the proposed memristor has much higher adjustability and diversity due to its controllable parameters N and M. This property is important for the generation of multi-scroll attractors. Then, the magnetized HNN is modeled and expressed by

$$\begin{cases} \dot{x}_1 = -x_1 + 2\tanh(x_1) - 0.8\tanh(x_2) + 0.7\tanh(x_3) \\ \dot{x}_2 = -x_2 + 3.5\tanh(x_1) + 1.6\tanh(x_2) + 1.5\tanh(x_3) \\ \dot{x}_3 = -x_3 - 2.6\tanh(x_1) + 1.2\tanh(x_2) + \tanh(x_3) - \mu W(\varphi)x_3 \\ \dot{\varphi} = cx_3 - dh(\varphi) \end{cases} \tag{5}$$

where $\mu W(\varphi)x_3$ is an electromagnetic induction current induced by electromagnetic radiation, μ represents feedback intensity of electromagnetic induction current, φ represents the magnetic flux across membrane of neuron 3, $W(\varphi)$ is used to describe the coupling between magnetic flux and membrane potential, c describes the contribution of magnetic flux on the formation of membrane potential. $-dh(\varphi)$ denotes the leakage of magnetic flux.

B. Equilibrium Point And Stability Analysis

The equilibrium points of the magnetized HNN can be solved by calculating the following equations

$$\begin{cases} -x_1 + 2\tanh(x_1) - 0.8\tanh(x_2) + 0.7\tanh(x_3) = 0 \\ -x_2 + 3.5\tanh(x_1) + 1.6\tanh(x_2) + 1.5\tanh(x_3) = 0 \\ -x_3 - 2.6\tanh(x_1) + 1.2\tanh(x_2) + \tanh(x_3) - \mu W(\varphi)x_3 = 0 \\ cx_3 - dh(\varphi) = 0 \end{cases} \tag{6}$$

Obviously, (6) is a fourth-order transcendental equation that is difficult to solve by conventional methods. Thus, (6) is solved by adopting MATLAB. Without loss of generality, $h(\varphi)$ with N=2 is considered as an example and other parameters are fixed as a=1, b=0.01, c=1, and d=1.2. (6) is changed as

$$\begin{cases} x_3 = dh(\varphi)/c \\ x_2 = \mathrm{atanh}((-x_1 + 2\tanh(x_1) + 0.7\tanh(x_3))/0.8) \\ f_1(\varphi, x_1) = -x_2 + 3.5\tanh(x_1) + 1.6\tanh(x_2) + 1.5\tanh(x_3) = 0 \\ f_2(\varphi, x_1) = \\ \quad -x_3 - 2.6\tanh(x_1) + 1.2\tanh(x_2) + \tanh(x_3) - \mu W(\varphi)x_3 = 0 \end{cases} . \tag{7}$$

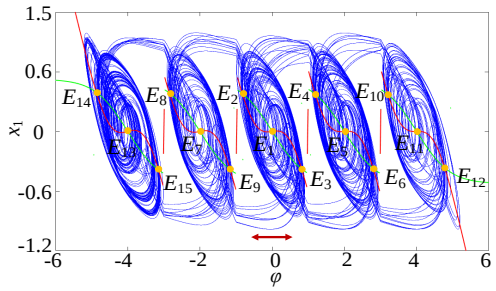

Fig. 2: Five-scroll attractor with fifteen equilibrium points (E_1-E_{15}) generated by $h_1(\varphi)$ with N=2.

The curves of both function $f_1(\varphi, x_1)$ in green and $f_2(\varphi, x_1)$ in red are drawn by using the graphic analytic method, as shown in Fig.2. It can be seen that there are fifteen intersections between the two curves. Taking the three equilibrium points [(-1.152, 0.384), (0, 0), (1.152, 0.384)] on the φ-x_1 plane in the middle as a guide, the equilibria expand to both sides along the direction of the arrow in red as the memristor control parameters alter. Based on Fig.2 and (7), the fifteen equilibrium points can be obtained. Nine equilibrium points are listed in TABLE I. The Jacobian matrix of each equilibrium point is calculated as

$$J = \begin{bmatrix} -1 + 2m_1 & -0.8m_2 & 0.7m_3 & 0 \\ 3.5m_1 & -1 + 1.6m_2 & 1.5m_3 & 0 \\ -2.6m_1 & 1.2m_2 & -1 + m_3 - \mu W(\varphi) & -\mu b x_3 \\ 0 & 0 & c & -d \end{bmatrix} \tag{8}$$

where m_i=sech$^2(x_i)$. The corresponding eigenvalues and stabilities are listed in TABLE I.

From TABLE I, there exist three types of equilibria: unstable index-1 saddle-foci, unstable index-2 saddle-foci and unstable foci. According to the Shilnikov theorem [25]: there exists self-excited chaos in a nonlinear system if there exists unstable saddle-foci. Here, scroll structures are yielded in the neighborhoods of unstable index-2 saddle-foci. And two sets of bond orbits are realized by an unstable index-1 saddle-focus and an unstable focus, respectively. That is to say, each index-2 saddle-focus corresponds to a scroll structure. Hence, five scrolls are generated in this situation, which is consistent with Fig.2. It is noted that the central scroll will be repeatedly constructed with increasing memristor control parameters. Indeed, when choosing a suitable memristive nonlinear function $h(\varphi)$, this proposed magnetized HNN can generate self-excited (2N+1)-scroll chaotic attractors (odd number) and (2M+2)-scroll chaotic attractors (even number).

III. Dynamics Analysis and Numerical Simulation

A. Multiple Coexisting Attractors

Let the parameters a=1, b=0.01, c=1, d=1.2, N=0 and make the memristor coupling strength μ as the adjustable parameter. When changing the parameter μ in the region [0.2, 1.2], the bifurcation diagrams of μ are numerically plotted in Fig.3(a), where the initial states are set to (0.1, 0.1, 0.1, 0.1) in pink and (-0.1, -0.1, -0.1, -0.1) in blue, respectively. Meanwhile, Fig.3(b) gives the Lyapunov exponents calculated using Wolf's Jacobian method, where only initial states (0.1, 0.1, 0.1, 0.1) are considered. It can be observed from Fig.3(a) that the magnetized HNN exhibits complex bifurcation behaviors including period, quasi-period, chaos, forward period-doubling bifurcation (FPDB), crisis scenarios (CS) as well as several periodic windows (PW). Moreover, multiple symmetric coexisting attractors can be

TABLE I: EQUILIBRIUM POINTS AND CORRESPONDING EIGENVALUES AND STABILITIES

Equilibrium points	Eigenvalues	Stability
E_7 (0,0,0,-2)	(-1.2, 0.9389, -0.1594±1.4580i)	Unstable index-1 saddle-focus
E_1 (0,0,0,0)	(-1.2, 0.9220, -0.1610±1.4446i)	Unstable index-1 saddle-focus
E_5 (0,0,0,2)	(-1.2, 0.9048, -0.1624±1.4337i)	Unstable index-1 saddle-focus
E_4 (0.384,0,0,0,1.152)	(0.4565±1.2548i, -1.3233, -1.0982)	Unstable index-2 saddle-focus
E_8 (0.384,0,0,0,-2.832)	(0.4615±1.2678i, -1.3274, -1.0995)	Unstable index-2 saddle-focus
E_2 (0.384,0,0,0,-0.816)	(0.4591±1.2615i, -1.3255, -1.0989)	Unstable index-2 saddle-focus
E_3 (-0.384,0,0,0,0.816)	(0.4628±1.2622i, -1.2242±0.1098i)	Unstable focus
E_9 (-0.384,0,0,0,-1.152)	(0.4699±1.2756i, -1.2389±0.1066i)	Unstable focus
E_6 (-0.384,0,0,0,2.832)	(0.4705±1.2709i, -1.2507±0.1006i)	Unstable focus

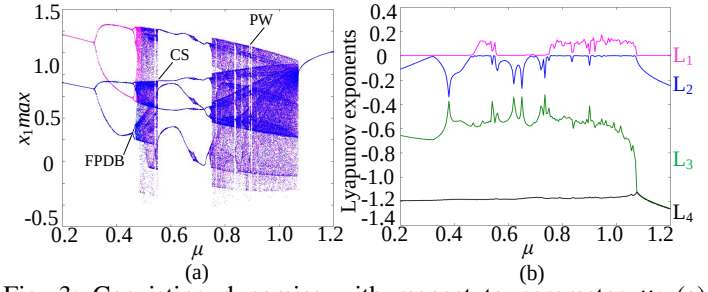

Fig. 3: Coexisting dynamics with respect to parameter μ: (a) coexisting bifurcation diagrams; (b) Lyapunov exponents.

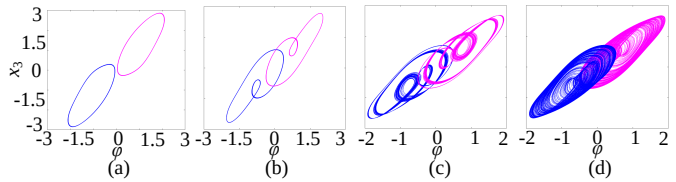

Fig. 4: Coexisting attractors with different values of parameter μ: (a) coexisting limit cycles at μ=0.2; (b) coexisting period-2 attractors at μ=0.4; (c) coexisting quasi-period attractors at μ=0.47; (d) coexisting chaos attractros at μ=0.48.

observed in the coexisting region of [0.2, 0.49]. Some typical symmetric coexisting attractors including coexisting limit cycles, coexisting period-2 attractors, coexisting quasi-period attractors and coexisting chaotic attractors are given in Fig.4.

B. Controllable n-Scroll Chaotic Attractors

Numerical simulations show that the magnetized HNN can generate any number of multi-scroll attractors. When the parameters are set as a=1, b=0.01, c=1, d=1.2, μ=1 and initial states (0.1, 0.1, 0.1, 0.1), n-scroll chaotic attractors can be generated by selecting different values of N or M in (4), as shown in Fig.5. Obviously, the number of scrolls generated by the magnetized HNN can be controlled by $2N$+1 and $2M$+2. To further reveal the complex chaotic dynamics, the Poincaré mappings on φ-x_1 and φ-x_3 phase planes for the 8-scroll attractor with x_2=0 are depicted in Fig.6(a) and (b), respectively. It can be seen from Fig.6 that the Poincaré mappings have irregular shapes, implying that the system generates extremely complex chaotic behavior. Furthermore, the first four Lyapunov exponents of the 8-scroll attractor are 0.1135, 0, -0.6442, -0.9825, respectively. The Kaplan-Yorke dimension of the 8-scroll attractor is calculated as 2.1762, which means the 8-scroll attractor is chaotic.

C. Initial Offset Boosting Behavior

When keeping the previous parameters unchanged except for M=5 and c=0.5 and the initial states are chosen as (0.1, 0.1, 0.1, 0.1, φ_0). When φ_0 varies in the range of [-8, 8], the bifurcation diagram of the state variable φ and the Lyapunov exponent spectrums are shown in Fig.7(a) and (b), respectively. As can be seen, in Fig.7(a), the bifurcation diagram exhibits multiple long strip-shaped regions with the same dynamical amplitude but different positions. Each of the long strip regions can evolve to be a 1-scroll attractor. Furthermore, it can be observed from Fig.7(b) that the magnetized HNN has invariant Lyapunov exponents, which means that it can produce continuously robust chaos. That is to say, the proposed magnetized HNN has complex initial offset boosting behavior highly dependent on initial states. Additionally,

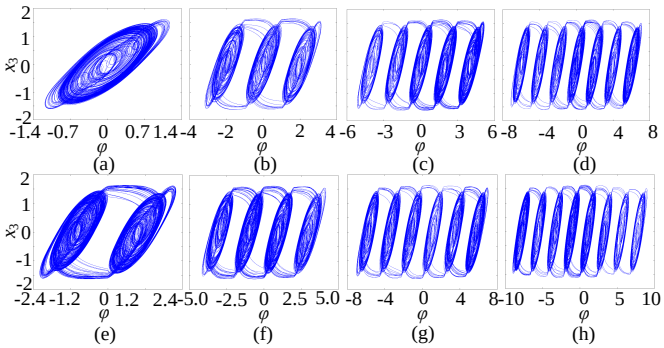

Fig. 5: n-scroll attractors with different values of N and M: (a) 1-scroll with N=0; (b) 3-scroll with N=1; (c) 5-scroll with N=2; (d) 7-scroll with N=3; (e) 2-scroll with M=0; (f) 4-scroll with M=1; (g) 6-scroll with M=2; (h) 8-scroll with M=3.

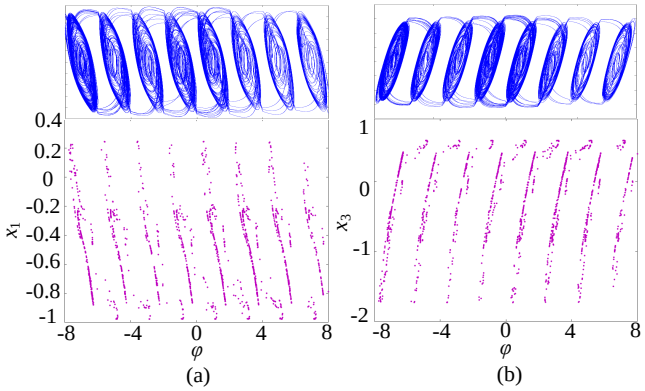

Fig. 6: Poincaré maps of 8-scroll attractor for x_2=0: (a) on φ-x_1 plane; (b) on φ-x_3 plane

with φ_0=±1, ±3, and ±5, the phase portrait of coexisting six 1-scroll attractors and corresponding time series of the state φ are given in Fig.8. In Fig.8(a), the six coexisting attractors are distributed along the φ-axis and have the same structure but different positions. Actually, infinitely many coexisting 1-scroll attractors can be generated as $N \to \infty$ and $M \to \infty$. Moreover, in Fig.8(b), the chaotic sequences are robust to retain chaos and their oscillation amplitudes can be nondestructively controlled by adjusting the memristor initial values. This property is very significant in practical applications because it can provide a large number of nondestructive and robust chaotic sequences for chaos-based secure communications.

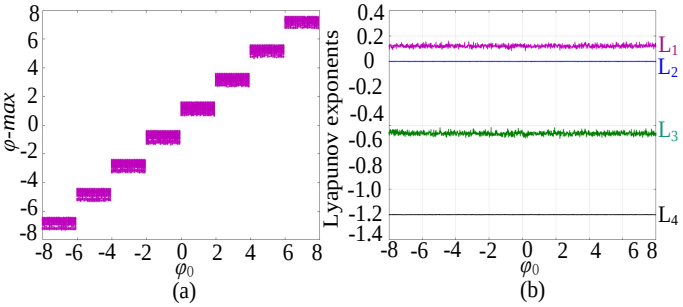

Fig. 7: Dynamics of the magnetized HNN for the memristor initial value φ_0: (a) bifurcation diagram; (b) Lyapunov exponents.

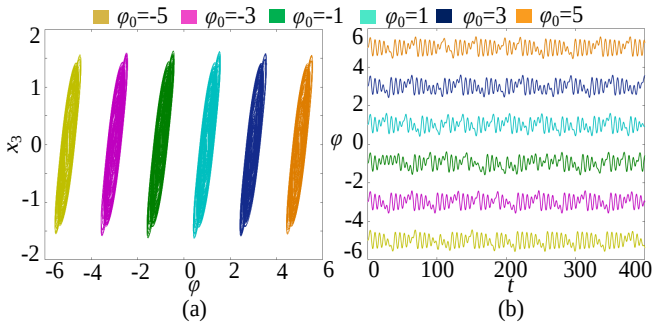

Fig. 8: The initial offset boosting behavior: (a) phase portrait of coexisting six chaotic attractors; (b) coexisting six chaotic sequences with different positions.

IV. Circuit Demonstration

A. Multisim Simulation

Before designing the magnetized HNN circuit, an improved multi-piecewise memristor circuit is introduced from reference [25], as shown in Fig.9. From Fig.9, the memristor circuit is made up of a nonlinear function generator circuit, an integration circuit, a multiplication circuit and an absolute value function circuit. Among them, the absolute value function circuit is introduced from reference [10]. S_1, S_2, $\cdots$, S_n are selection switches and e_1, e_2, $\cdots$, e_i are control voltages. By selecting different switches and appropriate control voltages, multi-scroll attractors with different number of scrolls can be realized as listed in TABLE II.

TABLE II: Different Number of Scroll with the Combination of the Switches and the Bias Voltages

S_1	S_2	S_3	$\cdots$	S_n	Number of scroll
e_1=1V	e_2=3V	e_3=5V	$\cdots$	e_i=(2n-1)V	
On	On	On	$\cdots$	On	1
On	Off	On	$\cdots$	On	3
On	Off	Off	$\cdots$	On	5
$\cdots$	$\cdots$	$\cdots$	$\cdots$	$\cdots$	$\cdots$
e_1=2V	e_2=4V	e_3=6V	$\cdots$	e_i=(2n)V	
Off	On	On	$\cdots$	On	2
Off	Off	On	$\cdots$	On	4
Off	Off	Off	$\cdots$	On	6
$\cdots$	$\cdots$	$\cdots$	$\cdots$	$\cdots$	$\cdots$

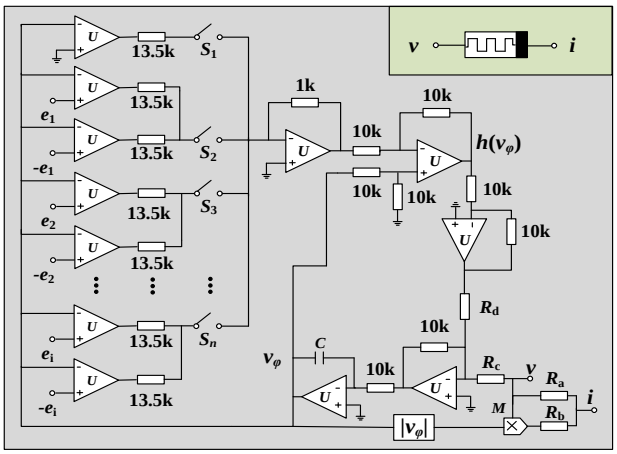

Fig. 9: Memristor circuit.

Furthermore, the circuit equation in Fig.9 can be written as

$$\begin{cases} i = (1/R_a + g|v_\varphi|/R_b)v \\ C\mathrm{d}v_\varphi/\mathrm{d}t = v/R_c - h(v_\varphi)/R_d \end{cases}, \tag{9}$$

where g=0.1 is the gain of the analog multiplier M, R_a=R/a, R_b=gR/b, R_c=R/c and R_d=R/d.

According to (5), the circuit of the magnetized HNN is designed in Fig.10, where the hyperbolic tangent function circuit from the reference [26] is adopted. Three output capacitor voltages v_1, v_2, v_3 denote three membrane potentials x_1, x_2, x_3, respectively. R_1-R_9 simulate nine fixed synaptic weight coefficients. The effect of electromagnetic induction is simulated by

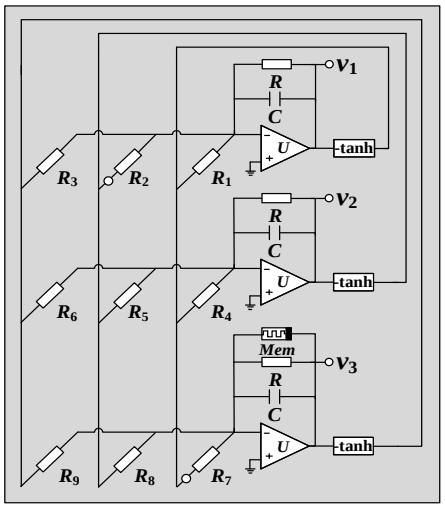

Fig. 10: Magnetized HNN circuit.

the memristor *Mem*. Based on the magnetized HNN circuit in Fig.10, the circuit state equations can be given by

$$\begin{cases} RC\dot{v}_1 = -v_1 + \frac{R}{R_1}\tanh(v_1) - \frac{R}{R_2}\tanh(v_2) + \frac{R}{R_3}\tanh(v_3) \\ RC\dot{v}_2 = -v_2 + \frac{R}{R_4}\tanh(v_1) + \frac{R}{R_5}\tanh(v_2) + \frac{R}{R_6}\tanh(v_3) \\ RC\dot{v}_3 = -v_3 - \frac{R}{R_7}\tanh(v_1) + \frac{R}{R_8}\tanh(v_2) + \frac{R}{R_9}\tanh(v_3) \\ -Rv_3(\frac{1}{R_a} + \frac{gv_\varphi}{R_b}) \\ RC\dot{v}_\varphi = \frac{R}{R_c}v_3 - \frac{R}{R_d}h(v_\varphi) \end{cases} \tag{10}$$

The designed magnetized HNN circuit is implemented in the Multisim simulation platform. Assuming that C=1 nF and R=10 kΩ and considering the fixed synaptic weight coefficients, resistors R_1-R_9 can be calculated as R_1=5 kΩ, R_2=12.5 kΩ, R_3=14.3 kΩ, R_4=2.85 kΩ, R_5=6.25 kΩ, R_6=6.66 kΩ, R_7=3.84 kΩ, R_8=8.33 kΩ, R_9=10 kΩ. Besides, R_a=$R/a\mu$, R_b=$gR/b\mu$, R_c=R/c and R_d=R/d. Numerous experiments show that the designed magnetized HNN circuit can generate results consistent with the numerical simulation results in section III. For example, for a=1, b=0.01, c=1, d=1.2, N=0, set R_c=10 kΩ and R_d=0.83 kΩ. Set two sets of initial voltages (0.1 V, 0.1 V, 0.1 V, 0.1 V) in pink and (-0.1 V, -0.1 V, -0.1 V, -0.1 V) in blue, respectively. For μ=0.2, 0.4, 0.47 and 0.48, respectively, when all switches are open, the Multisim simulation results of the coexisting attractors is depicted in Fig.11. For parameters a=1, b=0.01, c=1, d=1.2, μ=1, set R_a=10 kΩ, R_b=100 kΩ, R_c=10 kΩ and R_d= 8.33 kΩ. Set e_1=1 V and e_2=3 V. When S_2 and S_3 are off, the 5-scroll chaotic attractor is captured in Fig.12(a). Set e_1=2 V and e_2=4 V. When S_1, S_2 and S_3 are off, the 6-scroll chaotic attractor is captured in Fig.12(b). Set e_1=1 V, e_2=3 V and e_3=5 V. When S_2, S_3 and S_4 are off, the 7-scroll chaotic attractor is captured in Fig.12(c); Set e_1=2 V, e_2=4 V, e_3=6 V. When S_1, S_2, S_3 and S_4 are off, the 8-scroll chaotic attractor is captured in Fig.12(d). Obviously, the circuit simulation results are consistent well with the numerical simulation results in Fig.5. In addition, when keeping the previous circuit parameters unchanged except for R_c=20 kΩ. Set e_1=2 V, e_2=4 V, and e_3=6 V. The initial values of the four capacitors are set as 0.1 V, 0.1 V, 0.1 V, and v_φ, where v_φ=±1 V, ±3 V, and ±5 V. When S_1, S_2, S_3 and S_4 are off, the experimental results are given in Fig.13. As can be seen from Fig.13, the magnetized HNN generates coexisting six chaotic attractors and sequences under different initial capacitor voltages. That is to say, the magnetized HNN exhibits complex initial offset boosting behavior.

B. Circuit Experiment

Based on the circuits in Fig.9 and Fig.10, system (5) is physically implemented by using discrete active and passive electronic components including M/AD633JN and U/TL082CP. The circuit parameters are the same as the Multisim simulation. The obtained 3-scroll and 4-scroll attractors observed by the oscilloscope are shown in Fig.14. Clearly, the experimental results match those obtained from the MATLAB simulations. Through the circuit

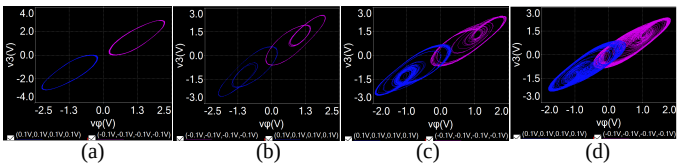

(a) (b) (c) (d)

Fig. 11: Multisim simulation results corresponding to numerical simulation results in Fig.4: (a) coexisting period attractors with R_a=50 kΩ and R_b=500 kΩ; (b) coexisting period-2 attractors with R_a=25 kΩ and R_b=250 kΩ; (c) coexisting quasi-period attractors R_a=21.5 kΩ and R_b=215 kΩ; (d) coexisting chaos attractros R_a=20.5 kΩ and R_b=200 kΩ.

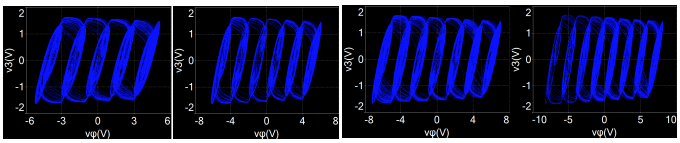

(a) (b) (c) (d)

Fig. 12: Multisim simulation results captured multi-scroll attractors from the magnetized HNN circuit: (a) 5-scroll attractor; (b) 6-scroll attractor; (c) 7-scroll attractor; (d) 8-scroll attractor.

experiment, it concluded that the physics-based multi-piecewise memristor model can be realized and can be applied to explore electromagnetic radiation. In addition, in this work, the memristor with nanoscale and low power is used to replace the nonlinear switching resistors. Thus, there is no need to design complex nonlinear switching circuits, which would reduce difficulties in circuit implementation.

V. Conclusion

In this brief, a memristor-based magnetized HNN with three neurons is constructed. Dynamical analysis and numerical simulation demonstrate that the multi-scroll chaotic attractors can be successfully generated from the magnetized HNN. And arbitrary number of multi-scroll attractors can be obtained by selecting suitable memristor control parameters. Meanwhile, the magnetized HNN can generate infinitely many coexisting attractors with the same topologies but different positions, which means that it has complex initial offset boosting behavior. Finally, some typical dynamical behaviors are successfully reproduced and verified based on the designed neural network circuit.

In the future, to obtain multi-direction or grid multi-scroll attractors, we may further consider the case that multiple neurons

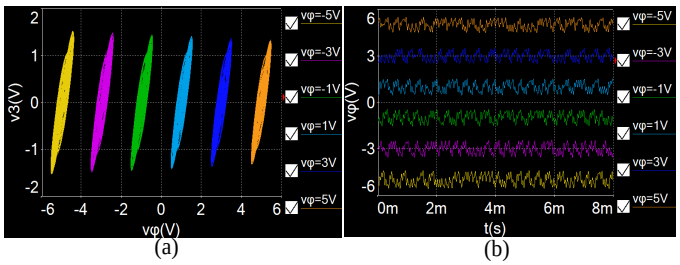

(a) (b)

Fig. 13: Multisim simulation results of initial offset boosting behavior corresponding to numerical simulation results in Fig.8.

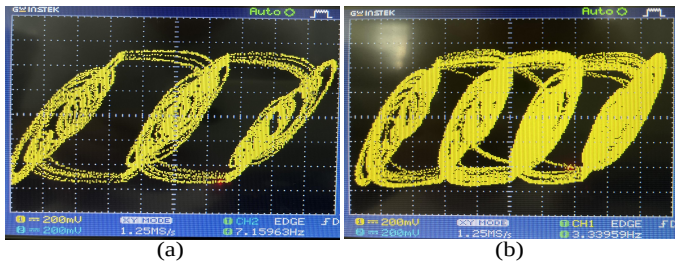

(a) (b)

Fig. 14: Experiment results. (a) 3-scroll attractor; (b) 4-scroll attractor.

of the HNN are influenced by electromagnetic radiation. In addition, we will use this magnetized HNN to further realize chaos-based engineering applications.

References

[1] E. N. Lorenz, "Deterministic nonperiodic flow," *J. Atmos. Sci*., vol. 20, no. 2, pp. 130-141, 1963.

[2] Q. Lai, Z. Wan, L. K. Kengne, et al., "Two-memristor-based chaotic system with infinite coexisting attractors," *IEEE Trans. Cir. Sys.-II: Brief Papers*., vol. 68, no. 6, pp. 2197-2201, 2020.

[3] W. S. Sayed, M. Roshdy, L. A. Said, et al., "Design and FPGA verification of custom-shaped chaotic attractors using rotation, offset boosting and amplitude control," *IEEE Trans. Cir. Sys.-II: Brief Papers*., vol. 68, no. 11, pp. 3466-3470, 2021.

[4] X. Zhang, C. Wang. "A novel multi-attractor period multi-scroll chaotic integrated circuit based on CMOS wide adjustable CCCII," *IEEE Access*., vol. 7, pp. 16336-16350, 2019.

[5] X. Ye, X. Wang, S. Gao, et al., "A new random diffusion algorithm based on the multi-scroll Chua's chaotic circuit system," *Opt. Lasers Eng*., vol. 127, p. 105905, 2020.

[6] J. Suykens, J. Vandewalle. "Quasilinear approach to nonlinear systems and the design of n-double scroll , no. n= 1, 2, 3, 4,…)," *IEE Proc.-Circuit Device Syst*., vol. 138, no. 5, pp. 595-603, 1991.

[7] Q. Hong, Y. Li, X. Wang, et al., "A versatile pulse control method to generate arbitrary multidirection multibutterfly chaotic attractors," *IEEE Trans. Comput-Aided Des. Integr. Circuits Syst*., vol. 38, no. 8, pp. 1480-1492, 2018.

[8] N. Wang, C. Li, H. Bao, et al., "Generating multi-scroll Chua's attractors via simplified piecewise-linear Chua's diode," *IEEE Trans. Circuits Syst. I-Regul. Pap*., vol. 66, no. 12, pp. 4767-4779, 2019.

[9] S. Zhang, C. Li, J. Zheng, et al., "Generating any number of initial offset-boosted coexisting chua's double-scroll attractors via piecewise-nonlinear memristor," *IEEE Trans. Ind. Electron*., vol. 69, no. 7, pp. 7202-7212, 2021.

[10] S. Yu, J. Lu, H. Leung, et al., "Design and implementation of n-scroll chaotic attractors from a general jerk circuit," *IEEE Trans. Circuits Syst. I-Regul. Pap*., vol. 52, no. 7, pp. 1459-1476, 2005.

[11] Q. Hong, Q. Wu, X. Wang, et al., "Novel nonlinear function shift method for generating multiscroll attractors using memristor-based control circuit," *IEEE Trans. Very Large Scale Integr. (VLSI) Syst*., vol. 27, no. 5, pp. 1174-1185, 2019.

[12] N. Wang, G. Zhang, H. Li. "Parametric control for multi-scroll attractor generation via nested sine-PWL function," *IEEE Trans. Cir. Sys.-II: Brief Papers*., vol. 68, no. 3, pp. 1033-1037, 2020.

[13] Y. Yang, L. Huang, J. Xiang, et al., "Three-dimensional sine chaotic system with multistability and multi-scroll attractor," *IEEE Trans. Cir. Sys.-II: Brief Papers*., vol. 69, no. 3, pp. 1792-1796, 2021.

[14] R. J. Escalante-González, E. Campos-Cantón. "A class of piecewise linear systems without equilibria with 3-D grid multiscroll chaotic attractors," *IEEE Trans. Cir. Sys.-II: Brief Papers*., vol. 66, no. 8, pp. 1456-1460, 2018.

[15] F. Wang, R. Wang, H. H. C. Iu, et al., "A novel multi-shape chaotic attractor and its FPGA implementation," *IEEE Trans. Cir. Sys.-II: Brief Papers*., vol. 66, no. 12, pp. 2062-2066, 2019.

[16] S. Zhang, C. Li, J. Zheng, et al., "Generating any number of diversified hidden attractors via memristor coupling," *IEEE Trans. Circuits Syst. I-Regul. Pap*., vol. 68, no. 12, pp. 4945-4956, 2021.

[17] D. Yan, M. Ji'e, L. Wang, et al., "Generating novel multi-scroll chaotic attractors via fractal transformation," *Nonlinear Dyn*., vol. 107, no. 4, pp. 3919-3944, 2022.

[18] J. A. K. Suykens, L. O. Chua. "n-double scroll hypercubes in 1-D CNNs," *Int. J. Bifurcation Chaos*., vol. 7, no. 08, pp. 1873-1885, 1997.

[19] H. Lin, C. Wang, C. Chen, et al., "Neural bursting and synchronization emulated by neural networks and circuits," *IEEE Trans. Circuits Syst. I-Regul. Pap*., vol. 68, no. 8, pp. 3397-3410, 2021.

[20] Z. T. Njitacke, S. D. Isaac, J. Kengne, et al., "Extremely rich dynamics from hyperchaotic Hopfield neural network, hysteretic dynamics, parallel bifurcation branches, coexistence of multiple stable states and its analog circuit implementation," *Eur. Phys. J.-Spec. Top*., vol. 229, no. 6, pp. 1133-1154, 2020.

[21] H. Lin, C. Wang, L. Cui, et al., "Brain-like initial-boosted hyperchaos and application in biomedical image encryption," *IEEE Trans. Ind. Inform*., vol. 18, no. 22, pp.8839-8850, 2022.

[22] C. Chen, J. Chen, H. Bao, et al., "Coexisting multi-stable patterns in memristor synapse-coupled Hopfield neural network with two neurons," *Nonlinear Dyn*., vol. 95, no. 4, pp. 3385-3399, 2019.

[23] H. Lin, C. Wang, Q. Hong, et al., "A multi-stable memristor and its application in a neural network," *IEEE Trans. Cir. Sys.-II: Brief Papers*., vol. 67, no. 12, pp. 3472-3476, 2020.

[24] H. Lin, C. Wang, W. Yao, et al., "Chaotic dynamics in a neural network with different types of external stimuli," *Commun. Nonlinear Sci. Numer. Simul*., vol. 90, p. 105390, 2020.

[25] S. Zhang, J. Zheng, X. Wang, et al., "Initial offset boosting coexisting attractors in memristive multi-double-scroll Hopfield neural network," *Nonlinear Dyn*., vol. 102, no. 4, pp. 2821-2841, 2020.

[26] Q. Lai, Z. Wan, H. Zhang, et al., "Design and analysis of multiscroll memristive hopfield neural network with adjustable memductance and application to image encryption," *IEEE Trans. Neural Netw. Learn. Syst*., DOI: 10.1109/TNNLS.2022.3146570, 2022.